ORIGINAL ARTICLE

International Journal of Applied Mathematics in Control Engineering

Journal homepage: http://www.ijamce.com

# Blast Furnace Condition Recognition Based on Improved GCN and Multi-Source Data Feature Fusion

**Zhiwei Zhao[1, 2, 3] | Qiqi Li[4] | Yadi Zhao[1, 2] | Tengfei Sun[5] | Song Liu[1, 2, 3]***

[1]Institute of Artificial Intelligence, Tangshan University, Tangshan, Hebei, 063000, China

[2]Tangshan Key Laboratory of New Technology of Internet of Things and Mobile Internet, Tangshan, Hebei, 063000, China

[3]Tangshan Key Laboratory of Indoor Positioning Technology, Tangshan, Hebei, 063000, China

[4]School of Metallurgy, Northeastern University, Shenyang, Liaoning, 110819, China

[5]Institute of Artificial Intelligence, North China University of Science and Technology, Tangshan, Hebei, 063000, China

**Correspondence**
S. Liu, Institute of Artificial Intelligence, Tangshan University, Tangshan, Hebei, 063000, China
Email: neversettle0722@163.com

**Article Info**
Article history:
Received 20 February 2025
Accepted 22 April 2025
Available online 25 April 2025

**Abstract**

To address the problem of imbalance of blast furnace furnace condition data categories, this study uses category-weighted cross-entropy loss function and synthetic minority oversampling technique in the training process of graph convolutional network, which improves the performance of graph convolutional network model, and effectively mitigates the negative impact of imbalance of furnace condition data categories on the training of the model. In order to comprehensively recognize the blast furnace furnace conditions, a multi-source data feature fusion method is proposed, which further improves the model performance by fusing the furnace condition numerical data, the air outlet image features and the furnace top image features. The experimental results show that the model recognizes the furnace conditions with an accuracy of 94.25% and an F1 score of 94.8%, realizing the recognition of blast furnace conditions based on multi-source data feature fusion.

**KEYWORDS**

Graph convolutional network, category-weighted cross-entropy loss function, synthetic minority oversampling technique, multi-source data feature fusion

## 1 | INTRODUCTION

As the mainstay of the national economy, the iron and steel industry is an important symbol of the country's economic level and comprehensive national strength. Blast furnace (BF) is one of the most important smelting equipments in the iron and steel industry, playing a key role in transforming iron ore into metallic iron [1]. Once the BF is started, it has to run uninterruptedly for years and years, and the deterioration of the BF condition will reduce the service life of the BF, which will cause huge losses if it reduces the production efficiency or jeopardizes the personal safety [2]. Therefore, it is crucial to grasp the BF condition correctly so that the staff can make timely adjustments to avoid the deterioration of the furnace condition.

Currently there are three main methods for determining the BF condition, which are: mechanism-based methods [3, 4], knowledge-based methods, and data-driven [5, 6] methods. The mechanism-based prediction method is to model the dynamics inside the BF [7] for the calculation of furnace heat index and other parameters. With the further knowledge of the internal structure of the BF and the improvement of the modeling technology, in order to be able to better respond to the situation inside

Digital Object Identifiers: 10.62953/IJAMCE.340425

the BF and guide the operation, many experts have successively proposed a lot of local models, such as: BF fabric [8], BF throat gas flow distribution model, soft melting zone model, furnace heat index prediction model, combustion zone model, and furnace cylinder and furnace bottom erosion model. However, the construction of mechanism models needs to be based on the laws of conservation of mass, momentum and energy, and the model formulas require close correlation with physical and chemical theories [9].

The knowledge-based approach is to transform subjective experience, knowledge, etc., into qualitative descriptions, and then, based on these descriptions, to analyze the actual situation in concrete terms and to judge the furnace conditions. The key is to use qualitative descriptions to accurately represent the complex logical relationships in the industrial production process, including the degree of relationship and mutual influence between different production links, and the flow sequence of reactant products. These are based on the operator's actual production and operation experience and theoretical knowledge, the need for experience, knowledge, and the relationship between the different links of the furnace to make a more accurate judgment. Existing knowledge-based methods are mainly expert systems, such as: Japan's Kawasaki AGS (Advance Go-Stop) system, Finland's Rautanrankki BF Control Expert System, voestalpine Optimization Control System for VAiron BF, Shougang's Artificial Intelligence BF Smelting Expert System. However, the application of expert systems relies on the acquisition of experts' domain knowledge, which is complex and profound and relies on the accumulation of staff's long-term experience, and it takes a lot of time to update the expert system with the changes in the operating environment [10].

The data-driven approach [11, 12] is the main way to judge the BF condition, and the data-driven model is to change the model based on the data, rather than to build the model after collecting and analyzing the data. BF is a black-box system with complex multiphase flow, heat and mass transfer, and accompanying high-temperature and high-pressure reactions [13], which leads to strong coupling between many parameters of the BF, and most of the existing data-driven models are only aimed at the prediction of a certain parameter of the BF, e.g., prediction of iron-silicon water content [14, 15], prediction of the iron and water temperature, prediction of the furnace temperature, and prediction of the differential pressure of the BF [16], permeability index prediction [17], gas utilization prediction, these studies are based on machine learning and deep learning methods, and the general process is as follows: firstly, do the correlation analysis to select the parameters with high correlation; then, downsize the selected parameters [18]; and finally, use the machine learning or deep learning methods to predict the BF parameters. Because the above BF parameters are continuous values, using the regression method [19, 20] can achieve good results, but in this study, the BF furnace conditions are labeled according to the expert rules, which are discrete values, so the regression [21, 22] method is not applicable, and this study proposes to use the classification method [23, 24] to identify the BF furnace conditions. Training a good classification model requires a category-balanced dataset, however, the BF operates stably all year round, and there is a lot of data in the normal category and very little data in the abnormal category, therefore, this study mitigates the imbalance of the categories of the BF furnace conditions in the dataset by changing the loss function and oversampling during the model training process.

In order to judge the furnace condition more comprehensively, this study not only uses numerical data, but also uses the image data at the BF air outlet and top furnace, which is also important for the judgment of the BF condition, and fuses the image data with the numerical data after feature extraction to realize the judgment of the BF condition based on the multimodal feature fusion [25]. Due to the complexity of the BF furnace condition, all parameters are important, therefore, this study does not do correlation analysis and dimensionality reduction operation [26], and all the parameters obtained are input into the deep learning model [27] for training. Automatically learning multi-level feature representations from raw data and capturing complex relationships and patterns without manually defining features are the advantages of deep learning [28].

## 2 | CONSTRUCTION AND PREPROCESSING OF DATASETS

### 2.1 | Numerical Data Acquisition

In this study, the actual production data of a BF was collected as the research basis, and the data contained a variety of key parameters related to the furnace condition, but among them, the iron content data was recorded in furnace times with time intervals ranging from 60 to 120 minutes, which resulted in the mismatch of its time frequency with that of the other production

data, and in order to ensure the unity of the time frequency, the time-alignment process of the iron content data was carried out in this study. Proximity interpolation was used to adjust the iron content data so that it was aligned with other production data on the time axis. After processing, 8781 production data were obtained, which included the parameters shown in Table 1.

**TABLE 1** BF parameters

| **BF Parameters** | | | |
|---|---|---|---|
| Cooling air volume | Gas utilization | Coal ratio | Iron temperature |
| Cold Air Pressure | Furnace belly gas volume | W value | CaO content |
| Hot air pressure | Oxygen enrichment rate | Hot air temperature | SiO2 content |
| Average pressure on top of the furnace | Furnace temperature difference | Cold air temperature | Al2O3 content |
| Differential pressure | Cooling wall temperature | Gas pressure | MgO content |
| Permeability index | Hourly material batch | Cross-measured temperature | FeO content |
| Oxygen | Furnace bottom pressure | Actual iron weight | TiO2 content |
| Hot air temperature | Differential pressure | Slag quantity | V2O3 content |
| Furnace top temperature | Upper differential pressure | Si content | Iron output |
| Actual air velocity | Bottom differential pressure | Mn content | Cooling wall temperature |
| Blast air humidity | Air volume | S content | Cr content |
| Kinetic energy of blast air | Gas utilization | P content | Coal injection amount |
| Mixed gas CO2 content | Oxygen enrichment | Ti content | Mixed gas H2 content |
| Mixed gas CO content | K value | C content | |

## 2.2 | Numerical Data Cleaning

In this study, columns with more than 20% missing values were removed, and for the remaining missing values [29], linear interpolation was used to fill in the missing values. The box plot method is used to deal with the abnormal values, and for the values judged to be abnormal by the box plot, they are first eliminated, and then filled [30] in using the mean, median, or interpolation method, in order to reduce the interference of the abnormal data on the training of the model, and at the same time to retain the overall trendiness of the data. In order to eliminate the scale difference between different parameters of the BF numerical data and improve the model's ability to learn various types of features, the Z-score standardization method is used to standardize the numerical data, and the standardization can transform all the features into a distribution with a mean of 0 and a standard deviation of 1, ensuring that the model can view all the features equally and improving the model convergence speed. The Z-score method is shown in equation (1):

$$z = \frac{x - \mu}{\sigma} \tag{1}$$

where $x$ is the value of the original feature; $\mu$is the mean value of the feature; $\sigma$ is the standard deviation of the feature $x$.

## 2.3 | Furnace Condition Category

According to the BF process as well as the experience of the staff, this study classifies the furnace condition categories into four categories, which are normal, to hot, to cool, and difficult to travel. The performance corresponding to each type of furnace

condition is as follows:

(1)During the normal operation of the BF, its air pressure and air volume remain stable, with almost no spikes or jagged fluctuations, and the permeability index is stable; the top temperature of the BF is maintained at about 200°C, and the temperature fluctuation is within 50°C; there is no spikes in the top pressure curve of the BF; the CO2 gas concentration in the throat area shows the distribution characteristics of high at the edges and low in the center; the temperatures of the slag and the iron are in the suitable range, and the fluidity of the iron is The temperature of slag and molten iron are in the appropriate range, and the fluidity of molten iron is good, and the content of silicon and sulfur is low; the imaging at the top of the BF shows that the center area is smooth and without disorder.

(2) The performance of the BF when the BF is to hot includes: the wind pressure rises gradually, accompanied by the wind volume decreases gradually; the permeability index decreases; the pressure difference between the upper part increases, the top pressure decreases, the temperature of the top of the furnace rises; the content of silicon increases, the temperature of molten iron increases, and the area of the air outlet is brighter than the normal state.

(3) The performance when the furnace temperature is to cool includes: the wind pressure decreases, the wind volume increases, the permeability index rises, and the roof temperature decreases. In addition, the slag and molten iron composition is also affected, which is manifested by the decrease of silicon content, the rise of sulfur content, and the increase of FeO content at the same time.

(4) When the furnace condition is difficult to travel, the performance is as follows: the falling speed of charge slows down; the wind pressure tends to increase while the wind volume decreases, and the two lose the coordination; the permeability index decreases; the temperature of the top of the furnace rises and the temperature curve becomes narrower.

The 8781 numerical data obtained were categorized according to expert experience and expert rules, and the amount of data for each type of furnace condition is shown in Table 2. As can be seen from Table 2, the data volume of the four categories is not balanced, and the normal category is predominant. In order to make the data categories tend to be balanced, this study does deletion of the data in the normal category, and the processing rule is: if the status of a row of data in the previous row and the next row are both normal, the data in that row can be deleted. This method ensures that the deleted data will not affect the overall trend of furnace conditions, while effectively reducing the amount of redundant data in the normal category. The amount of data in each category after processing is shown in Table 3. Although the amount of data in the normal category has been significantly reduced compared to Table 2, the data categories are still unbalanced, therefore, this study proposes a GCN model that incorporates the category-weighted cross-entropy [29] loss function and synthetic minority oversampling technique (SMOTE) [30] to mitigate the adverse effects of data category imbalance on model training.

**TABLE 2** Data amount corresponding to each category of furnace conditions

| Furnace condition | Amount of data |
|---|---|
| Normal | 8354 |
| To hot | 100 |
| To cool | 104 |
| Difficult to travel | 223 |
| All | 8781 |

## 2.4 | Construction of A Dataset of Air Outlet and Furnace Top Images Corresponding to Numerical Data

In this section, according to the moment columns in the preprocessed numerical data, the BF air outlet image and the furnace top image at the corresponding moments are collected respectively, and two independent datasets are constructed: the BF air outlet image dataset and the furnace top image dataset, with 1061 images in each dataset. The image size was uniformly adjusted to 224×224 pixels and normalized.

**TABLE 3** Table 2 Data amount corresponding to each category of furnace conditions

| Furnace condition | Amount of data |
|---|---|
| Normal | 634 |
| To hot | 100 |
| To cool | 104 |
| Difficult to travel | 223 |
| All | 1061 |

## 3 | MODELING METHODOLOGY

### 3.1 | BF Condition Recognition Model

In order to alleviate the adverse effects of data category imbalance on model training, this study proposes a BF condition identification model based on improved graph convolutional network (GCN), named Graph Convolutional Network with Class and Synthesis (GCNCS). GCNCS is based on GCN with the introduction of class-weighted cross-entropy loss function and SMOTE. function and SMOTE, naming the GCN with only the category-weighted cross-entropy loss function as Graph Convolutional Network with Class (GCNC).

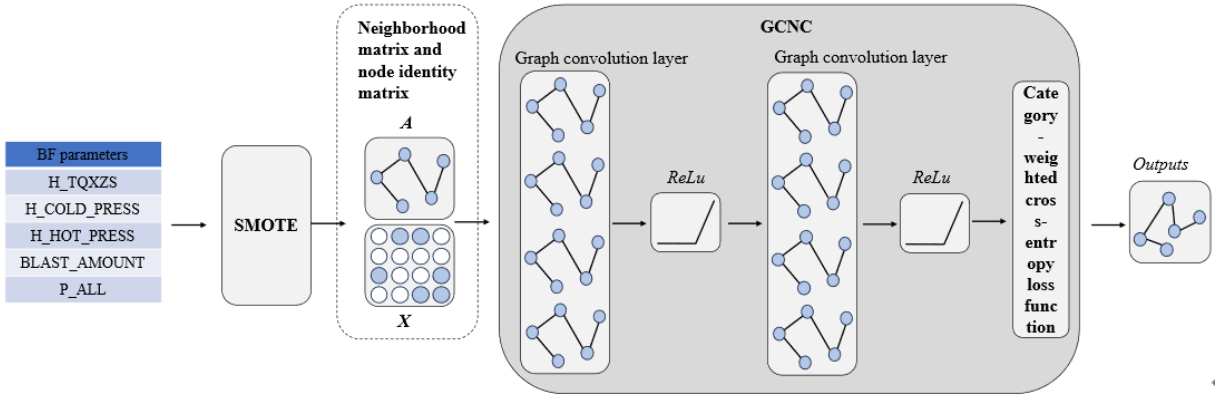


**FIGURE 1** Structure of the GCNCS model

The structure of GCNCS is shown in Fig. 1, and its main process is as follows: firstly, the numerical data of BF furnace conditions are input, and divided into training set and test set in the ratio of 7:3; then the minority class samples in the training set are expanded by using SMOTE to enhance the learning effect of the model on the minority class samples; then, the graph structure and adjacency matrix are constructed in order to classify the samples by using the GCNC; finally, the data are fed into the GCNC for training to learn the complex relationships and patterns of furnace data. The core elements in GCNCS are described in the follow-up of this section.

#### 3.1.1 | Graphical Structure

A common graph structure contains nodes and edges [31], as shown in Fig. 2, defined as, where denotes the set of nodes, denotes the set of edges connected between nodes, nodes represent entities, and edges denote relationships between entities. Each node has a feature vector that represents the attribute or state of the node. The connection relationships between nodes are described by adjacency matrices, and these nodes and connection relationships are input into GCNC for computation and analysis together in the form of feature vectors and adjacency matrices. Assuming that the number of vertices in the graph structure is n,

then the adjacency matrix is an n × n matrix, and if there is a relationship between the nodes, it is represented as 1 in the adjacency matrix, and if there is no connection, it is 0. In this study, the furnace conditions are classified according to the change of the BF parameters in the current moment and the previous moment, and there is a relationship between the BF parameters at the current moment and the BF parameters at the previous moment, therefore, the current moment and the previous moment are treated as two nodes, and construct edges between the two nodes as shown in equation (2).

$$A_{ij} = \begin{cases} 1, (V_{i-1}, v_i \in E) \\ 0, else \end{cases} \tag{2}$$

where: $A_{ij}$ is neighborhood matrix; $V_{i-1}$is previous node, corresponding to the previous row of data;,$v_i$is the current node, corresponding to the current row of data.

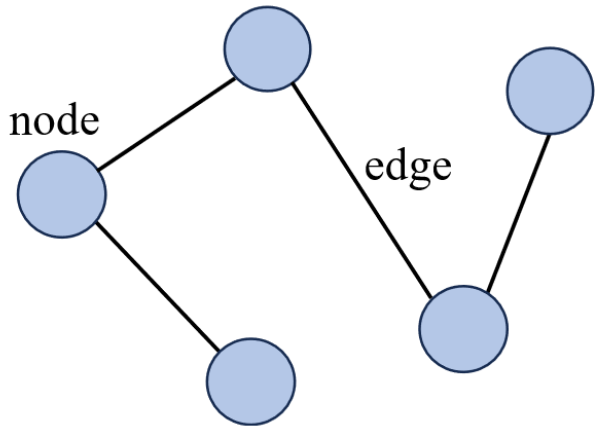


**FIGURE 2** Structure of the GCNCS model

### 3.1.2 | GCN

GCN [32] is a typical representative of Graph Neural Networks (GNN) [33], is a deep learning model for graph structured data, which learns node representations by performing convolutional operations in graph structured data, aiming to perform tasks such as node classification, graph classification, link prediction, and so on, by aggregating the information of the nodes and their neighbors. The core idea of GCN is to aggregate the feature representations of each node with its neighbor nodes' feature representations are aggregated and the node's representation is learned through the topology of the graph. The new representation of each node is the result of weighted summation of the representations of its neighbor nodes, usually with its own original features. In Fig. 1 $A$ is the adjacency matrix, which represents the connection relationship between the nodes in the graph structure, and $X$ is the node feature matrix, which contains the original features of each node, and the graph convolution operation of each layer can be shown by equation (3).

$$H^{(l+1)} = \sigma(\hat{A}H^{(l)}W^{(l)}) \tag{3}$$

where: $\sigma$ is ReLu activation function; $\hat{A}$ is Normalized adjacency matrix; $H^{(l)}$ is Nodal feature representation of layer ($H^{(0)=X}$); $W^{(l)}$ is the weights of the $l$ layer.

### 3.1.3 | SMOTE

SMOTE is a common technique for dealing with class imbalance problems, especially for increasing the number of minority class samples in the training data. It increases the sample size of the minority class by synthesizing new minority class samples instead of simply copying the minority class samples, thus reducing the overfitting problem and improving the model's predictive

ability for the minority class. The idea of SMOTE is to generate new minority class samples by interpolation. The process can be divided into the following steps:

(1) Select a minority class sample, and for each minority class sample, find its nearest neighbor.

(2) Generate a new sample. Select a neighbor $x_{neighbor}$ randomly from the selected $k$ neighbors, then generate a new sample $x_{new}$ through linear interpolation. The new sample is generated by scaling the difference between the original sample $x$ and its neighbors $x_{neighbor}$ . The formula is shown in equation (4).

$$x_{new} = x + \lambda (x_{neighbor} - x) \tag{4}$$

where: $\lambda$ is a random number in the interval [0,1] is used to control the interpolation ratio.

(3) Repeat to generate samples. Repeat steps (1) and (2) for each minority class sample until the desired number of new samples are generated.

In this way, SMOTE generates new samples based on the original minority class samples and expands the sample space of the minority class, which improves the learning ability of the minority class during model training.

### 3.1.4 | Category-weighted Cross-entropy Loss Function

In order to minimize the impact of category imbalance, category-weighted cross-entropy is used as a loss function, which is an extension of the traditional cross-entropy loss function designed to deal with category imbalance. In the task of category imbalance, some categories have far more samples than others, causing the model to prefer predicting more categories. By setting different weights for different categories, it can help the model to pay more attention to a few categories, thus improving the prediction performance of the few categories. The traditional cross-entropy loss function is a common loss function used for classification problems, as shown in equation (5), and the category-weighted cross-entropy loss function is shown in equation (6).

$$L_{CE} = -\sum_{i=1}^{C} y_i \log(\hat{y}_i) \tag{5}$$

$$L_{CWCE} = -\sum_{i=1}^{C} \beth_i y_i \log(\hat{y}_i) \tag{6}$$

where: $C$ is number of categories; $y_i$ is real labels; $\hat{y}_i$ is the prediction result of the model; $w_i$ is the weights of the categories.

This study calculates the weight of each category based on the inverse proportionality method of the sample size of the categories, which is based on the idea that the categories with a larger sample size will be given a smaller weight and the categories with a smaller sample size will be given a larger weight. This is shown in equation (7).

$$w_i = \frac{1}{N_i + \varepsilon} \tag{7}$$

where: $N_i$ is the Number of samples for category $i$ ; $\varepsilon$ is a very small constant to avoid division by zero (in this paper it is 10-6). Finally, the weights are normalized to ensure that the weights of all categories add up to 1.

## 3.2 | Multi Source Data Feature Fusion

In this study, two ResNet18 [34] models are trained on the BF air outlet and furnace top image datasets with accuracies of 98.07% and 85.2%, respectively. The features of BF air outlet and furnace top images in Section 2.4 are extracted using the trained models, respectively. Accordingly, this study proposes a multi-source data feature fusion method for the task of recognizing BF conditions, aiming at effectively integrating the information from image data and numerical data to improve the model's ability to recognize BF conditions. The proposed multi-source data feature fusion method is shown in Fig. 3, and the flow is as follows:

1) Air outlet image feature extraction: use the trained air outlet image model to extract the features of the images in the air outlet image data set constructed in section 2.4 to obtain the features of the air outlet image;

2) Furnace top image feature extraction: use the trained furnace top image model to extract the features of the images in the

furnace top image data set constructed in section 2.4 to obtain the features of the furnace top image;

3) Feature fusion: the extracted features of the two parts of the BF image as BF parameters are fused with the numerical data to construct a numerical dataset after feature fusion, which provides more comprehensive input information for the furnace condition recognition model.

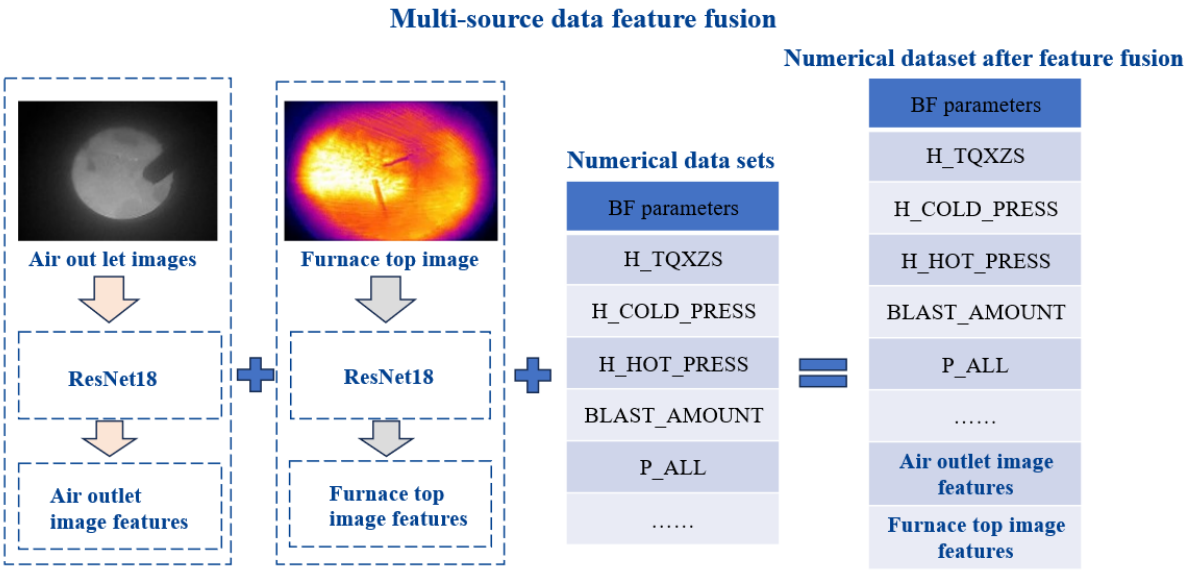


**FIGURE 3** Schematic diagram of feature fusion

## 4 | EXPERIMENTAL RESULTS AND ANALYSIS

The experiments were conducted on a computer with a CPU of Intel(R) Core(TM) i7-7700HQ @2.80GHz, 16GB of RAM, a GPU of NVIDIA GeForce GTX 1050, and a system of Windows 10. The models are built based on Python's PyTorch. The models include GCNCS, Transformer, Long Short-Term Memory (LSTM), GCNC, and GCN. The comparison experiment is to verify the ability of different models to recognize the BF conditions, and the models include GCNCS, Transformer, and LSTM; and the ablation experiment is to verify the category-weighted cross-entropy loss function and the effectiveness of SMOTE, the models include GCNCS, GCNC, GCN. Epoch is set to 100 for the training of each model; the optimization algorithm is stochastic gradient descent; the optimizer is Adam; the batch size is set to 32; and the learning rate is set to 0.01. In the training of the GCNCS model, in order to avoid that the over-generation of SMOTE distorts the original data and the distribution characteristics, the generated data of each model are used as a basis for the comparison between the different models and the SMOTE. distribution features, the number of each minority class sample it generates is set to 50% of the original minority class sample number.

In this study, accuracy, precision, recall, and F1score are used as the evaluation metrics of the model, as shown in Eq. (8)-(11):

$$accuracy = \frac{T_P}{T_P + F_P + T_N + F_N} \tag{8}$$

$$precision = \frac{T_P}{T_P + F_P} \tag{9}$$

$$recall = \frac{T_P}{T_P + F_N} \tag{10}$$

$$Flscore = \frac{2 \times precision \times recall}{precision + recall} \tag{11}$$

where $T_P$ is the number of correctly identified positive examples, i.e., correctly identified, $F_P$ is the number of incorrectly identified positive examples, i.e., incorrectly identified; $T_N$ is the number of correctly identified negative examples; and $F_N$ is the number of incorrectly identified negative examples. In addition, the time required by the model to process each piece of data is also used as an evaluation metric in this study.

## 4.1 | Model Comparison Experiments

In order to verify the ability of different models to recognize the BF conditions, this subsection conducts comparative experiments on the BF numerical dataset constructed in Section 2.4, where the first 70% of the numerical dataset is used as the training set and the second 30% as the test set. Accuracy, precision, recall, F1 score, and the time required to process each piece of data during model training are used as the evaluation metrics of the models.

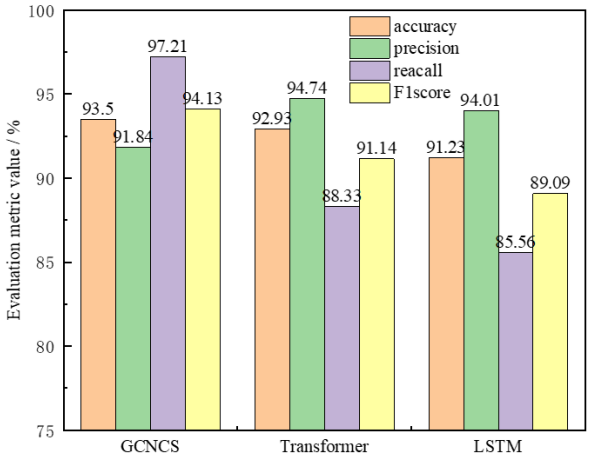


**FIGURE 4** Ablation experiment evaluation metric values for each model

The experimental results of each model in the test set are shown in Fig. 4, and the time required to process each piece of data during training is shown in Table 4. Comparing GCNCS and Transformer, it can be seen that although Transformer is 2.9 percentage points higher than GCNCS in terms of precision, GCNCS is 0.57, 8.88, and 2.99 percentage points higher than Transformer in terms of accuracy, recall, and F1 score, and 20.27ms less in terms of the time required to process each piece of data; comparing GCNCS and LSTM, it can be seen that although LSTM is 5.19ms less than GCNCS in terms of time needed to process each piece of data and 2.17 percentage points higher in terms of accuracy, GCNCS is 2.27, 11.65, and 5.04 percentage points higher than LSTM in terms of accuracy, recall, and F1 scores, respectively.

Comparison results show that GCNCS is more capable of classifying the overall data than Transformer and LSTM; in the category-imbalanced BF numerical dataset, the precision of GCNCS decreases compared to Transformer and LSTM suggesting that GCNCS produces more false positives in recognizing more minority class samples, misclassifying some majority class samples as minority classes; The improved recall rate indicates that GCNCS has a stronger ability to capture the minority classes that are otherwise difficult to recognize and reduces the leakage; the improved F1 score indicates that GCNCS achieves a better balance between reducing false alarms and avoiding leakage. In contrast, the GCNCS model has better overall performance and is more suitable for the furnace condition recognition task.

## 4.2 | Model Ablation Experiments

In order to verify the effectiveness of the category-weighted cross-entropy loss function and SMOTE in GCNCS, this subsection conducts ablation experiments on the BF numerical dataset constructed in Section 2.4, where the first 70% of the

**TABLE 4** Time required to process each piece of data for each model in the comparison experiment

| Model | Time required to process each piece of data / ms |
|---|---|
| GCNCS | 5.99 |
| Transformer | 26.26 |
| LSTM | 0.8 |

numerical dataset is used as the training set and the second 30% as the test set. Accuracy, precision, recall, F1 score, and the time required to process each piece of data during model training are used as the evaluation metrics of the model.

The experimental results of each model in the test set are shown in Fig. 5, and the time required to process each data during training is shown in Table 5. Based on the results of GCNCS and GCNC, it can be seen that GCNCS outperforms GCNC by 1.66, 1, 0.24, and 0.68 percentage points in terms of accuracy, precision, recall, and F1 score, respectively. This is because GCNCS introduces SMOTE on the basis of GCNC, which expands the representation space of minority classes at the data distribution level by synthesizing minority class samples in the training set, enabling the model to access richer minority class data, thus further improving the model performance. Correspondingly, the increase in the amount of data in the minority class leads to a larger number of nodes in the graph structure and a larger graph structure size so that the GCNCS model takes more time to process each piece of data than the GCNC during training, but it is within the acceptable range.

The experimental results of each model in the test set are shown in Fig. 5, and the time required to process each data during training is shown in Table 5. Based on the results of GCNCS and GCNC, it can be seen that GCNCS outperforms GCNC by 1.66, 1, 0.24, and 0.68 percentage points in terms of accuracy, precision, recall, and F1 score, respectively. This is because GCNCS introduces SMOTE on the basis of GCNC, which expands the representation space of minority classes at the data distribution level by synthesizing minority class samples in the training set, enabling the model to access richer minority class data, thus further improving the model performance. Correspondingly, the increase in the amount of data in the minority class leads to a larger number of nodes in the graph structure and a larger graph structure size so that the GCNCS model takes more time to process each piece of data than the GCNC during training, but it is within the acceptable range.

Based on the results of GCNC and GCN, it can be seen that although GCN is 3.41 percentage points higher than GCNC in terms of precision, GCNC is 1.32, 10.89, and 3.9 percentage points higher than GCN in terms of accuracy, recall, and F1 score, respectively. The high precision indicates that GCNC is more capable of classifying the overall data, the low precision indicates that GCNC introduces a certain degree of false positives in recognizing the minority class samples, and the increase in recall reflects that GCNC improves the recognition of the minority class and reduces the number of missed detections. This performance of "decreased precision and increased recall" is mainly due to the introduction of the category-weighted cross-entropy loss function in the loss function of GCNC, which improves the model's focus on minority samples, which further leads to the improvement of the F1 score, reflecting that it has reached a better balance between precision and recall.

**TABLE 5** Time required to process each piece of data for each model of the ablation experiment

| Model | Time required to process each piece of data / ms |
|---|---|
| GCNCS | 5.99 |
| GCNC | 2.61 |
| GCN | 2.57 |

Based on the results of GCNCS and GCN, it can be seen that although GCN is 2.41 percentage points higher than GCNCS in terms of precision, GCNCS is 1.89, 11.13, and 4.58 percentage points higher than GCN in terms of accuracy, recall, and F1 score, respectively. The high accuracy rate indicates that GCNCS has better overall classification ability, and the high F1 score indicates that GCNCS achieves a better trade-off between precision and recall. Overall, GCNCS outperforms GCN, which demonstrates

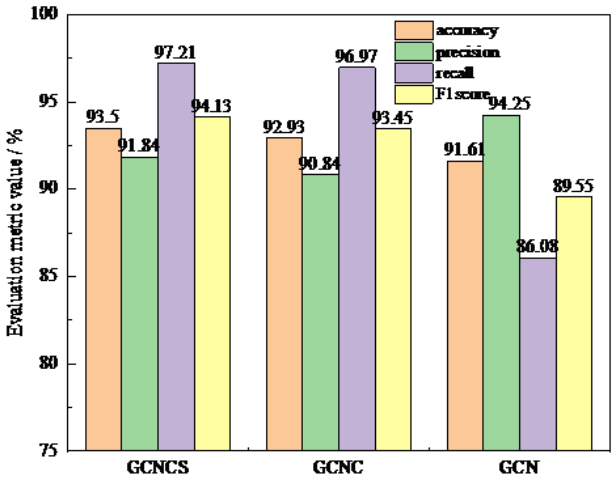


**FIGURE 5** Ablation experiment evaluation metric values for each model

the effectiveness of the category-weighted cross-entropy loss function and SMOTE in mitigating category imbalance. In view of the excellent performance of the GCNCS model in the experiments, GCNCS will be selected as the BF condition identification model for subsequent experiments.

## 4.3 | Comparison Experiment Before and After Feature Fusion

In order to verify the effectiveness of the feature fusion method, this subsection uses the numerical datasets before and after feature fusion of multi-source data to train the GCNCS model and perform comparative analysis, respectively. Among them, the numerical dataset before feature fusion is the numerical dataset constructed in Section 2.4, while the numerical dataset after feature fusion contains the feature information of the air outlet image and the furnace top image. The effectiveness of the multi-source data feature fusion method is demonstrated by comparing the experimental results on the two datasets. Both datasets are divided into training and test sets in the ratio of 7:3. The evaluation metrics are accuracy, precision, recall, and F1 score. The experimental results are shown in Fig. 6.

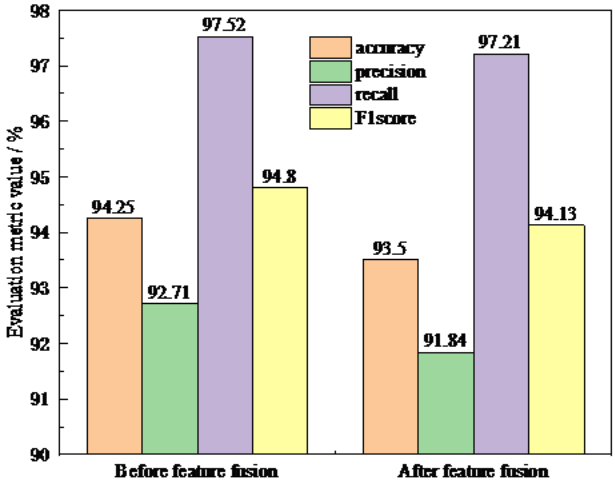


**FIGURE 6** Evaluation metric value of GCNCS before and after feature fusion

As can be seen in Fig. 6, the numerical dataset using feature fusion achieves 94.25%, 92.71%, 97.52%, and 94.8% in terms of accuracy, precision, recall, and F1 score, which are 0.75, 0.87, 0.31, and 0.67 percentage points higher than that of the numerical dataset before the use of feature fusion, respectively. This is due to the fact that feature fusion integrates features from

different sources, including numerical data, air outlet image features, and furnace top image features, forming a multi-dimensional information complementary to each other, which further improves the performance of the model in furnace condition recognition and proves the effectiveness of the feature fusion method.

In this study, an improved GCN model and a multi-source data feature fusion method are proposed around the BF condition recognition task. For the problem of data category imbalance, the model introduces category-weighted cross-entropy loss function and SMOTE, which effectively alleviates the negative impact of data category imbalance on model training. In addition, more comprehensive feature information is constructed by fusing the numerical data of furnace condition, air outlet image features and furnace top image features, which further improves the recognition ability of the model. The experimental results show that the improved method achieves 94.25% accuracy and 94.8% F1 score on the furnace condition recognition task, which verifies the enhancement of the model performance by the fusion of multi-source data features, and provides a new way of thinking for metallurgical enterprises to comprehensively recognize the BF condition.

## 5 | CONCLUSION

Aiming at the category imbalance problem in the furnace condition numerical data, an improved GCN model is proposed, i.e., the category-weighted cross-entropy loss function is introduced into the GCN model and combined with SMOTE, which effectively mitigates the adverse effect of category imbalance on model training.

In addition, in order to fully utilize the multi-source information during BF operation, the study proposes a multi-source data feature fusion method, which fuses the numerical data of furnace conditions, air outlet image features, and furnace top image features, so as to make the feature information of the furnace conditions richer and more comprehensive, and thus further improve the model performance.

The experimental results show that the proposed method achieves 94.25% accuracy and 94.8% F1 score in the furnace condition recognition task, realizing the BF condition recognition based on feature fusion of multi-source data, which is of great significance in guiding the intelligent recognition of BF conditions.

## ACKNOWLEDGEMENT

The authors gratefully acknowledge the financial support provided by the Natural Science Foundation of Hebei Province (E2024105036), the Tangshan Talent Funding Project (B202302007, A2021110015).

## DECLARATION OF COMPETING INTEREST

The authors declare that they have no known competing financial/commercial interests or personal relationships that could have appeared to influence the work reported in this paper.

## REFERENCES

[1] Y.H. Shi, S.H. Zhang, X.J. Liu, et al. Blast furnace differential pressure prediction based on XGBoost-BP fusion model with SSA optimization[J]. Journal of Iron and Steel Research, 2024, 36(08): 1019-1033.
[2] G.M. Cui, C.L. Yan, Y.H. Guan. Prediction of cooler and hotter blast furnace conditions based on support vector machine[J]. Journal of Iron and Steel Research, 2024, 36(08): 1019-1033.
[3] L. Zhao, J.C. Yan, R.L. Xie, et al. Catalysis mechanism of solution loss reaction of metallurgical coke in blast furnace: Experimental and modeling study[J]. Fuel, 2021, 290: 120025.
[4] M. Liu. China's blast furnace ironmaking technology development direction of the pipe view[J]. Ironmaking, 2021, 40: 1-6.
[5] H.W. Li, X. Li, X.J. Liu, et al. Evaluation and Prediction Models for Blast Furnace Operating Status Based on Big Data Mining[J]. Metals, 2023, 13(7): 1250.
[6] J.P. Li, C.C. Hua, X.P. Guan. Modeling of large-scale blast furnace smelting process based on mechanism, data and knowledge[J]. Journal of Shanghai Jiaotong University, 2018, 52(10): 1142-1154.
[7] J.Y. He, C. Zou, J.X. Zhao, et al. Kinetic study on thermal analysis of non-isothermal/isothermal combustion of charcoal and pulverized coal for blast furnace blowing[J]. Coal Conversion, 2022, 45(04): 34-45.

[8] J.S. Chen, H.B. Zuo, Q.G. Xue, et al. A review of burden distribution models of blast furnace[J]. Powder Technology, 2022, 398: 117055.
[9] J. Zhang. Deep learning-based modeling and prediction of blast furnace conditions[D]. Changsha University Of Science Technology, 2021.
[10] J.Z. Zhao. Research on the diagnosis method of blast furnace condition based on improved PCASVM[D]. Northeastern University, 2020.
[11] Q. Shi, J. Tang, M.S. Chu. Process metallurgy and data-driven prediction and feedback of blast furnace heat indicators[J]. International Journal of Minerals, Metallurgy and Materials, 2024, 31(6): 1228-1240.
[12] Y. Luo, X.M. Zhang, KANO M, et al. Data-driven soft sensors in blast furnace ironmaking: a survey[J]. Frontiers of Information Technology Electronic Engineering, 2023, 24(3): 327-354.
[13] S.B. Kuang, Z.Y. Li, A.B. Yu. Review on modeling and simulation of blast furnace[J]. Steel research international, 2018, 89(1): 1700071.
[14] X.J. Liu, Y. Deng, X. Li, et al. Prediction of silicon content in blast furnace molten iron based on big data technology[J]. China Metallurgy, 2021, 31(02): 10-16.
[15] Z.H. Jiang, C. Xu, W.H. Gui, et al. Prediction method of silica content in blast furnace molten iron based on optimal working condition migration[J]. Acta Automatica Sinica, 2022, 48(01): 194-206.
[16] D.W. Jiang, Z.Y. Wang, K.J. Li, et al. Machine Learning Models for Predicting and Controlling the Pressure Difference of Blast Furnace[J]. JOM, 2023, 75(11): 4550-4561.
[17] X.J. Liu, T.S. Li, X. Li, et al. Prediction of Blast Furnace Gas Permeability Index Based on KPCA-CNN-LSTM Modeling[J]. Metallurgical Industry Automation, 2024, 48(02): 103-113.
[18] W.K. Jia, M.L. Sun, S.J. Hou, et al. Feature dimensionality reduction: a review[J]. Complex Intelligent Systems, 2022, 8(3): 2663-2693.
[19] Y. Ren, Y.D. Tu, Y.P. Yi. Balanced predictive regressions[J]. Journal of Empirical Finance, 2019, 54: 118-142.
[20] Flavio S. V. Gomes , Klaus F. Coco , Jose Leandro Felix Salles. Multistep forecasting models of the liquid level in a blast furnace hearth[J]. IEEE Transactions On Automation Science And Engineering, 2016, 14(2): 1286-1296.
[21] GOMES F S, CôCO K F, SALLES J L F. Multistep forecasting models of the liquid level in a blast furnace hearth[J]. IEEE Transactions On Automation Science And Engineering, 2016, 14(2): 1286-1296.
[22] K. Guo, Y.X. Zhang, S. Zhang, et al. Classification model for blast furnace status based on multi-source information[J]. Engineering Applications of Artificial Intelligence, 2024, 141: 109728.
[23] Y.C. Zong, S.W. Hu, D.B. Qin, et al. Iron-Tapping State Recognition of Blast Furnace Based on Bi-GRU Composite Model and Post-Processing Classifier[J]. IEEE Sensors Journal, 2023, 23(18): 22006-22018.
[24] Z.Y. Ren, Z.C. Wang, Z.W. Ke, et al. An overview of multimodal data fusion[J]. Computer Engineering and Applications, 2021, 57: 49-64.
[25] JIA W, SUN M, LIAN J, et al. Feature dimensionality reduction: a review[J]. Complex Intelligent Systems, 2022, 8(3): 2663-2693.
[26] Mohammed A, Kora R. A comprehensive review on ensemble deep learning: Opportunities and challenges[J]. Journal of King Saud University-Computer and Information Sciences, 2023, 35(2): 757-774.
[27] J. Zhao, S.F. Chen, X.J. Liu, et al. Outlier screening for ironmaking data on blast furnaces[J]. International Journal of Minerals, Metallurgy and Materials, 2021, 28(6): 1001-1010.
[28] Y.T. Jin, Y.J. Zhang, X.J. Liu, et al. Blast furnace gas utilization prediction based on EEMD-BAS-RBF[J]. Journal of Iron and Steel Research, 2023, 35(11): 1330-1338.
[29] Y.X. Wu, K. Du, X.J. Wang, et al. Misclassification-guided loss under the weighted cross-entropy loss framework[J]. Knowledge and Information Systems, 2024, 66: 4685-4720.
[30] Karim El Moutaouakil, Mouhamed Roudani, Abdellatif El Ouissari. Optimal entropy genetic fuzzy-C-means SMOTE (OEGFCM-SMOTE)[J]. Knowledge-Based Systems, 2023, 262: 110235.
[31] X.P. Liu, Q.Y. Zheng, X.L. Zhu. A study of graphical neural networks in materials chemistry[J]. Chemistry, 2024, 87(11): 1309-1318.
[32] L.Q. Feng, Y.Q. Zhao, W.X. Zhao, et al. A comparative review of graph convolutional networks for human skeleton-based action recognition[J]. Artificial Intelligence Review, 2022, 55: 4275-4305.
[33] G. Gkarmpounis, C. Vranis, N. Vretos, et al. Survey on Graph Neural Networks[J]. IEEE Access, 2024, 12: 128816-128832.
[34] Asad Ullah, Hassan Elahi, Zhaoyun Sun, et al. Comparative analysis of AlexNet, ResNet18 and SqueezeNet with diverse modification and arduous implementation[J]. Arabian journal for science and engineering, 2022, 47(2): 2397-2417.

**Zhiwei Zhao** graduated from Yanshan University in 2012 with a Ph.D. degree in control science and engineering. Currently, he is the director of Institute of Artificial Intelligence, Tangshan University. His main research interests are artificial intelligence and strip rolling. In the past five years, as a project leader, he has presided over one Natural Science Fund project of Hebei Province, one Provincial Science and Technology Plan project of Hebei Province, one Key Project of Hebei Education Department, one Youth Fund project of Hebei Education Department, two Science and Technology Plan projects of Tangshan City, one Doctoral Innovation Fund, and one subject of Tangshan Research Institute of Southwest Jiaotong University, and participated in one National Natural Science Foundation of China project.

**Qiqi Li** is currently pursuing a PhD degree at the School of Metallurgy, Northeastern University. His main research interests are energy saving and emission reduction in steel manufacturing.

**Yadi Zhao** graduated from Taiyuan University of Science and Technology with a bachelor's degree in automation in 2013, and earned a master's degree in control science and engineering from North China University of Science and Technology in 2019. She is currently a lecturer at Tangshan University. Her main research areas include intelligent manufacturing and data analysis.

**Tengfei Sun** is currently pursuing his degree in Institute of Artificial Intelligence, North China University of Science and Technology. His main research interests are in the target optimization of blast furnace ironmaking.

**Song Liu** received the B.S. in Information and Computing Science from Hebei United University in 2013, followed by M.S. and Ph.D. degrees in Metallurgical Engineering from North China University of Science and Technology in 2013 and 2020. He's currently an associate professor at Tangshan University, having pursued a postdoctoral degree at Tangshan Iron and Steel Group in 2022. With 30+ publications in esteemed journals, he holds three national invention patents and two utility model patents. He presided over 5 provincial and municipal directive projects and 3 enterprise horizontal projects. His research involves metallurgical intelligent manufacturing, data mining, and image recognition.